

FIELD ENHANCED PHOTOCATALYTIC INACTIVATION OF ESCHERICHIA  
COLI USING IMMOBILIZED TITANIUM DIOXIDE NANOTUBE ARRAYS

by

Jeffrey M. Huber

A thesis submitted to the faculty of  
The University of Utah  
in partial fulfillment of the requirements for the degree of

Master of Science

Department of Civil and Environmental Engineering

The University of Utah

May 2015

Copyright © Jeffrey M. Huber 2015

All Rights Reserved

**UNIVERSITY OF UTAH GRADUATE SCHOOL**

**STATEMENT OF THESIS APPROVAL**

The thesis of Jeffrey M. Huber

Has been approved by the following supervisory committee members:

Otakuye Conroy-Ben, Chair 03/03/2015  
Date Approved

Steven Burian, Member 03/03/2015  
Date Approved

Swomitra Mohanty, Member 03/03/2015  
Date Approved

Krista Carlson, Member 03/03/2015  
Date Approved

and by Michael Barber, Chair of  
the Department of Civil and Environmental Engineering.

and by David B. Kieda, Dean of The Graduate School.

## ABSTRACT

A batch reactor device utilizing photocatalysis and a flow reactor combining photocatalysis and photoelectrocatalysis were developed for bacterial disinfection in lab-synthesized and natural waters. The batch reactor provided a 90% decrease in initial concentration ( $\sim 1 \times 10^3$  CFU/mL) after 60 minutes when subjected to incident light at  $100 \text{ mW/cm}^2$  and continuous mixing via aeration. A combination of photocatalysis and photoelectrocatalysis in the flow reactor provided complete inactivation of contaminated waters with flow rates of 50 mL/min. Both devices consisted of immobilized titanium dioxide nanotube arrays as the catalyzing medium. The flow reactor used an applied bias of up to 6 V without noticeable water splitting. Light intensity, applied voltage, and background electrolytes and concentration were all found to impact the device performance. Complete inactivation of *E. coli* W3110 (800 CFU/mL) occurred in 15 seconds in the flow reactor irradiated at  $25 \text{ mW/cm}^2$  with an applied voltage of 4 V in a 100 ppm NaCl solution. Disinfection in natural water was inhibited by the presence of inorganic ions and other constituents that are commonly found in natural water. To simulate natural scenarios in which a point-of-use device might be employed, testing was conducted in a natural environment using source water from Emigration Creek in Salt Lake City, Utah. A higher voltage of 6 V was required to reach 100% inactivation in

natural surface water. The nanotube flow through disinfection chamber shows promise as a personal point-of use device for *E. coli* inactivation.

## TABLE OF CONTENTS

ABSTRACT.....	iii
LIST OF FIGURES .....	vii
ACKNOWLEDGEMENTS.....	viii
1. INTRODUCTION .....	1
1.1 Problem Statement .....	1
1.2 Titanium Dioxide as a Photocatalyst.....	2
1.3 History of Titanium Dioxide as a Photocatalyst .....	4
1.4 Disinfection Mechanism of Photocatalysis .....	5
1.5 Project Description .....	8
1.6 Research Questions .....	9
2. BACKGROUND/LITERATURE REVIEW .....	12
2.1 Photocatalysis Using TiO <sub>2</sub> Nanotubes.....	12
2.2 Photocatalytic and Photoelectrocatalytic Inactivation of Bacteria.....	14
2.3 Photocatalytic and Photoelectrocatalytic Oxidation in the Presence of Inorganic Ions .....	16
3. EXPERIMENTAL METHODS AND MATERIALS .....	17
3.1 Device Fabrication .....	17
3.2 <i>E. coli</i> Preparation .....	18
3.3 <i>E. coli</i> Inactivation .....	18
3.4 <i>E. coli</i> Analysis .....	19
3.5 Natural Water Disinfection .....	20
4. RESULTS .....	26
4.1 TNA Appearance.....	26
4.2 Inactivation Performance in a Polycarbonate Batch Reactor.....	26
4.3 Inactivation Performance in a Flow Reactor.....	27

5. DISCUSSION .....	38
5.1 Inactivation Mechanism .....	38
5.2 Electroporation .....	39
5.3 Ion Effect on Disinfection .....	41
5.4 Combined PC and PEC .....	42
6. CONCLUSIONS.....	43
6.1 Analysis Results .....	43
6.2 Future Research.....	44
LITERATURE CITED .....	46

## LIST OF FIGURES

1. Schematic describing the electron-hole pair formation when subjected to irradiation.	11
2. Synthesis setup for TiO <sub>2</sub> fabrication. ....	21
3. Schematic of the batch reactor device used for PC inactivation.....	22
4. Batch reactor with TNA mesh. Mixing is achieved via aeration in the reactor.....	23
5. Schematic of the flow reactor used for photoelectrocatalytic inactivation.....	24
6. Setup used in the flow reactor experiments .....	25
7. Top view SEM image of nanotubes annealed in nitrogen/2% hydrogen blend on the titanium wire used in the flow reactor experiments.....	30
8. Side view SEM image of nanotubes annealed in a nitrogen/2% hydrogen blend on the titanium wire used in the flow reactor device experiments. ....	31
9. Batch reactor experiments with irradiation at 100 mW/cm <sup>2</sup> .....	32
10. Bacterial inactivation performance under 15 second and 60 second contact times subjected to 100 mW/cm <sup>2</sup> in the flow-through device.....	33
11. Bacterial inactivation performance under simulated conditions for 0 mW/cm <sup>2</sup> , 25 mW/cm <sup>2</sup> , and 100 mW/cm <sup>2</sup> showing the effect that different levels of inactivation have on the system.....	34
12. Bacterial inactivation performance using Al and TNA anode materials .....	35
13. Bacterial inactivation performance using different NaCl concentrations under 100 mW/cm <sup>2</sup> irradiation.....	36



## ACKNOWLEDGEMENTS

I would like to thank my thesis advisor, Dr. Otakuye Conroy-Ben, and thesis committee member, Dr. Steven Burian, for their guidance and support throughout the duration of this project. I would also like to thank committee members, Dr. Swomitra Mohanty and Dr. Krista Carlson, for all of their time spent assisting in the lab and providing endless amounts of expert advice. Finally, I would like to thank my friends and family for the endless amount of support they have provided throughout my college career. Financial support for this research came from the Utah Science Technology and Research (USTAR) initiative, the State of Utah Governor's Office for Economic Development's (GOED) Technology Commercialization & Innovation Program (TCIP) and the University of Utah Research Foundation.

## CHAPTER 1

### INTRODUCTION

#### 1.1 Problem Statement

Every year, more than 800,000 people die from water, sanitation, and hygiene-related causes and one in nine people lack access to drinking water worldwide (Tropical Medicine and International Health 2014), accounting for approximately 800 million people as of 2015. Almost 2.5 billion people do not have access to adequate sanitation (UN Water 2013). Currently, there is no universally affordable method of water treatment available to mitigate this problem.

In the United States we are not immune to contaminated water. There are an estimated 240,000 water main breaks per year in the US. Failures in drinking water infrastructure can result in water disruptions and impediments to emergency response (ASCE 2014). Contaminated wells, natural disasters and dilapidated infrastructure are all reasons to have a point of use (POU) water disinfection system. Fortunately, with the advancements in water treatment technologies, we are getting closer to mitigating these issues, reducing the incidence of water-borne illnesses, and making sanitation and clean drinking water more universally available. Solar-driven water treatment is a strong focus in developing regions as they tend to lack electricity and the necessary infrastructure that is available in the US.

According to the Outdoor Industry Association more than 140 million Americans make outdoor recreation a priority in their daily lives, including 82% of Utah residents (~2.4 million people) (Outdoor Industry Association 2014). Much of this recreation is expected to require the consumption of water from natural sources that have the potential to contain bacteriological contaminants such as *Escherichia coli* (*E. coli*); harmful itself and an indicator of the presence of other disease-causing bacteria. Although there are a variety of proven alternatives for purifying source water available in the outdoor recreation industry, they have their disadvantages. The technology described herein utilizes a solar-driven oxidation reaction to inactivate bacteria rather than chemical oxidation (extended treatment times and unpleasant taste), physical filtration (costly pumping, need to replace filters), or ultraviolet disinfection (expensive parts) in currently available commercial products. Table 1 shows the characteristics of each of the existing treatment methods. The photocatalytic (PC) titania used for the reaction is nontoxic and nonconsumable so there is no need for replacement unless the device is physically damaged.

### 1.2 Titanium Dioxide as a Photocatalyst

Titanium dioxide ( $\text{TiO}_2$ ) is a solid-state photocatalyst that produces reactive oxygen species (ROS) when exposed to ultraviolet radiation (UV) (<387 nm) (Fujishima 1972). When  $\text{TiO}_2$  is irradiated with sunlight, electron-hole pairs are generated and react with water molecules, forming ROSs, such as  $\bullet\text{OH}$  radicals, and bacterial inactivation occurs via physical destruction of the cell membrane (Matsunaga 1985, Palaez 2012).  $\text{TiO}_2$  induced PC inactivation has been studied with both suspended and immobilized

nanoparticles (Rincon 2003, Alrousan 2009, Kim 2013, Wu 2008, Wolfrum 2002, Sunada 2003, Wei 1994, Matsunaga 1995). Rincon et al. found that suspended  $\text{TiO}_2$  nanoparticles (TNPs) had slightly higher biocidal activity rates than Nafion® supported TNP coated membranes. It was suggested that the support structure could have played a role in the recombination of the electron-hole pairs, which would lead to lower radical formation and biocidal activity (Rincon 2003). However, immobilization of  $\text{TiO}_2$  is typically preferred if the material and device are to be reused, as TNP suspensions can be difficult to implement into devices where separation of the material from the water is needed before consumption.

#### *1.2.1 Titanium Dioxide Nanotube Array Formation*

Inherently immobilized  $\text{TiO}_2$  nanotubes can be easily formed through the anodization of titanium metal. Anodically formed  $\text{TiO}_2$  nanotube arrays (TNAs) are also beneficial as they can be created on any titanium morphology, which also provides better connectivity to the metal substrate (Nie 2014, Butterfield 1997, Smith 2013). Connectivity is especially important in a photoelectrocatalytic (PEC) cell, where an anodic bias is applied to the titanium substrate of the TNA for improved efficiency. Driving photogenerated electrons away from the surface reduces electron-hole pair recombination, increasing the time and concentration of holes that can react with water molecules to form radicals or directly oxidize bacteria. It also prevents the TNA from becoming negatively charged, eliminating any electrostatic repulsion that the negatively charged bacteria would have to overcome (Gerischer 1993).

### *1.2.2 Device Development for Real World Application*

Consumer devices using this technology have not yet been established due to long treatment times (typically observed in batch reactors) or low throughput (i.e., microfluidic chambers). This research has led to the development of an economical device that is ideal for portable, POU applications, such as backpacking. The following reports the study on a flow reactor that combines PEC inactivation with electroporation for the inactivation of *E. coli* W3110. Parameters such as contact time, lighting conditions, applied voltage and NaCl concentrations were investigated. Additionally, in situ testing was conducted at Emigration Creek at Rotary Glen Park in Salt Lake City to evaluate the efficacy of the system in a real-world setting with natural surface water.

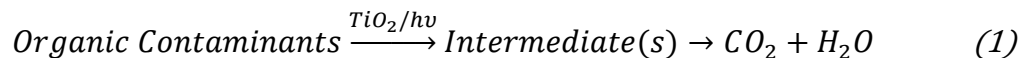
### 1.3 History of Titanium Dioxide as a Photocatalyst

Research in the field of photocatalysis with TiO<sub>2</sub> electrodes began as early as 1972 when Fujishima and Honda discovered PC water splitting (Fujishima and Honda 1972). When they discovered water could be split into hydrogen and oxygen, many studies were focused on hydrogen generation for energy purposes. Later studies discovered the catalytic power of certain semiconductors when subjected to irradiation (Fox and Dulay 1993). Some semiconductors were found to completely mineralize certain environmental pollutants (Fujishima et al 2007). While a number of studies were carried out using WO<sub>3</sub>, SiO<sub>2</sub>, ZrO<sub>2</sub>, ZnO, Nb<sub>2</sub>O<sub>3</sub>, Fe<sub>2</sub>O<sub>3</sub>, among other semiconductors, TiO<sub>2</sub> has become the preferential semiconductor for solar irradiated photolysis for a number of reasons. TiO<sub>2</sub> is the most active photocatalyst under the photon energy of 300 nm <  $\lambda$  < 390 nm and remains stable after catalytic cycles (Chong 2010). TiO<sub>2</sub> has a high

resistance to photocorrosion and an ideal band-gap energy (Ye and Ohmori 2002). It is also a desirable material due to its abundance, chemical inertness, and durability (Saravanan 2009) and nontoxic properties. Following Fujishima and Honda's discovery, many studies sought to better understand the fundamental processes and improve the PC efficiencies of  $\text{TiO}_2$  (Linsebigler 1995). Matsunaga et al. first reported the PC inactivation of microorganisms using UV-irradiated  $\text{TiO}_2$  powder (Matsunaga et al. 1988). Since then, significant research has been conducted in the area of environmental cleanup and water disinfection using  $\text{TiO}_2$  photocatalysis. In particular, active interest in bacterial inactivation has been shown in many recent studies (Alrousan 2009, Rincon 2003, Nie 2014, Baram 2011, Markowska-Szczupak 2011, Foster 2011, Dalrymple 2010, Lu 2003, Cho 2004). These discoveries could potentially open the door to cost effective chemical-free water purification for a number of applications (personal POU, residential, commercial, municipal, and industrial). Furthermore, advancements in the formation and manipulation of TNAs have driven research in their use for water disinfection.

#### 1.4 Disinfection Mechanism of Photocatalysis

Contrary to current methods of water purification systems, photocatalysis breaks down pollutants into harmless substances and does not leave behind any byproducts to be disposed of. This is especially beneficial at a larger scale such as municipal or industrial water treatment plants due to the significant cost saving associated with waste disposal. Organic contaminants are mineralized to carbon dioxide and water via Eq. 1 (Chong 2010).

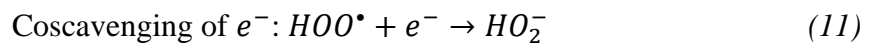
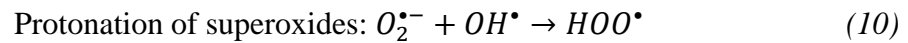
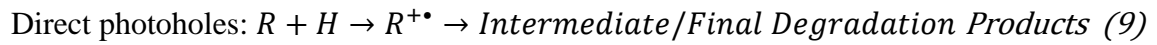
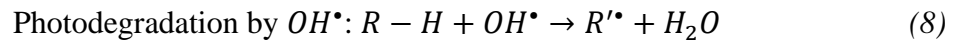
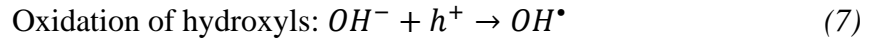
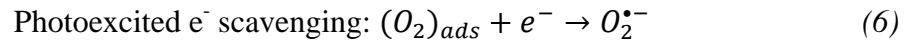
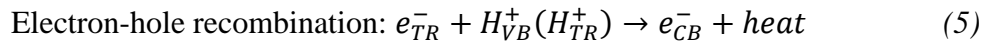
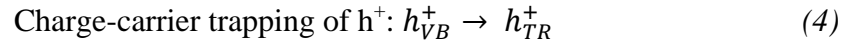
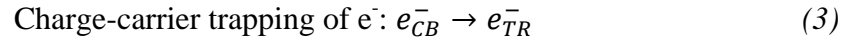
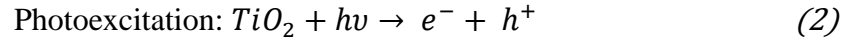


Disease-causing bacteria is oxidized without the introduction of chemicals such as chlorine, which is known to generate harmful disinfection byproducts such as trihalomethanes, haloacetic acids and chlorite.

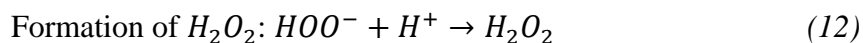
Advanced oxidation processes (AOPs) are an emerging technology that has shown promise in water treatment technologies. AOPs utilize the production of hydroxyl radicals to oxidize organic contaminants. For applications in water treatment, AOPs usually refer to processes involving  $\text{O}_3$ ,  $\text{H}_2\text{O}_2$  or UV light. AOPs also include semiconductor catalysis, cavitation, E-beam irradiation, and Fenton's reaction (Fox & Dulay 1993, Legrini 1993). Heterogeneous photocatalysis has received increased attention due to a number of important features extending their feasible applications in water treatment, such as ambient operating temperature and pressure, complete mineralization of compounds without generating secondary pollution, and low operating costs (Chong 2010).

The fundamental mechanism of photocatalysis with TNAs is the generation of oxidative and reductive reactions on its surface. This is contributed to the single electron in the  $\text{TiO}_2$  outer orbital. When photon energy equal to or greater than the bandgap of  $\text{TiO}_2$  is illuminated on its surface, the lone electron is photoexcited to the empty conduction band and leaves behind a hole in the valence band, creating an electron-hole pair ( $\text{e}^- - \text{h}^+$ ). The oxidation-reduction reactions that occur on the  $\text{TiO}_2$  surface upon illumination are shown in Eqs. 2-12. The bandgap of  $\text{TiO}_2$  is 3.2 eV and 3.0 eV for the anatase and rutile phase, respectively (Chong 2010). Figure 1 shows the electron-hole

pair formation when the  $\text{TiO}_2$  surface is subjected to adequate irradiation. The necessary wavelength required for these reactions is  $\lambda < 400 \text{ nm}$ .







### 1.5 Project Description

This thesis seeks to develop a point-of-use (POU) water disinfection device that can inactivate bacteria in natural surface waters utilizing solar irradiated photocatalysis coupled with a low applied voltage. The combination of photocatalysis and a low applied voltage is novel in this field of study and has shown promise as a potential technology suitable for personal use water disinfection systems. Although studies have been conducted on the inactivation of bacteria using semiconductor photocatalysis and photoelectrocatalysis, research has not evaluated this process on a large enough scale for personal use applications.

Immobilized TNAs submerged in a contaminated solution act as a catalyst when subjected to visible light irradiation. The energy from the sun generates electron-hole pairs needed to oxidize organic compounds into harmless end products and inactivate bacteria through physical destruction of the cell membrane. Applying an external voltage to the system further increases the efficiency of the system. An applied voltage initiates the generation of a major reactive species,  $h^+$ , further contributing to the direct oxidation and also suppresses the electron-hole pair recombination extending the life of the hole for increased oxidation. Laboratory testing has also indicated the possible occurrence of electroporation allowing the reactive species to penetrate bacterial cell walls attacking the interior of the cells resulting in quicker inactivation.

To determine the feasibility of the proposed technology for use as a real world water treatment application, batch reactor and flow reactor prototypes were developed for

testing and laboratory controlled experiments took place. Appropriate water chemistries were synthesized to harbor laboratory grown *E. coli* and simulate natural surface water chemistries. A variety of experiments were conducted under varying conditions and controlled settings. Natural water taken from Emigration Creek at Rotary Glen Park in Salt Lake City, Utah was also used for testing and the water chemistry and enumerated bacterial composition analyses were conducted by ChemTech-Ford Laboratories in Sandy, Utah. In situ pH, conductivity, temperature and ORP field data were also collected.

### 1.6 Research Questions

1. Determine the appropriate bacterial loading and water chemistry for experimentation.
2. Determine which parameters, such as irradiation intensity, contact time and applied voltage, have a noticeable effect of device performance.
3. Determine the optimal parameters, such as irradiation intensity, contact time and applied voltage to achieve complete biocide.
4. Determine optimal device design for effective biocide in a portable POU disinfection device.

Table 1. Comparison of water disinfection systems.

	<b>Filters</b>	<b>UV</b>	<b>Iodine/Chlorine</b>
Mechanism	Physically blocks agents	Alters cellular components	Chemical sterilization
Effective against	Bacteria Protozoa	Bacteria Protozoa Viruses	Bacteria Protozoa (some) Viruses
Treatment time (per liter)	< 1 minute	1.5 minutes	5 minutes to 4 hours
Investment / Volume treated	\$60+ / 1,000 – 5,000 L	\$90+ / 4,000 L	< \$0.50 / 1 L
Weight	10+ oz	5+ oz	< 1 oz
Disadvantages	Breakable components. Requires replacement parts.	Easily breakable. Requires batteries.	Poor taste. Chemical expiration. Consumed.

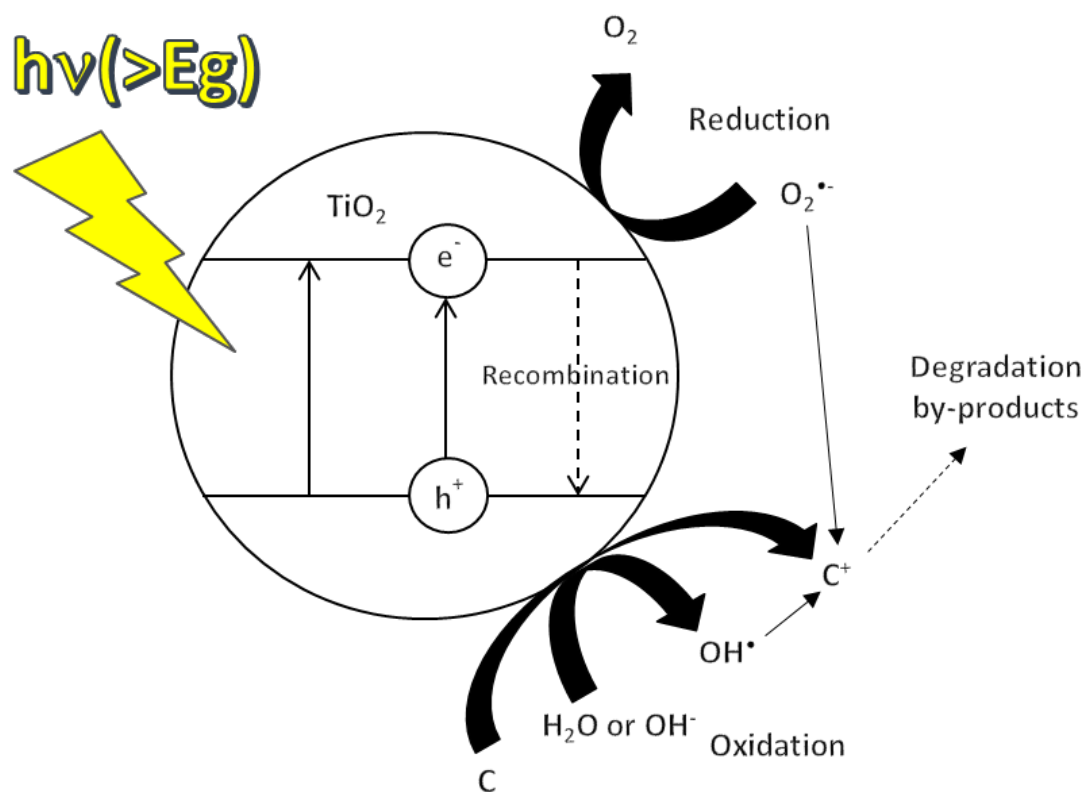


Figure 1. Schematic describing the electron-hole pair formation when subjected to irradiation.

## CHAPTER 2

### BACKGROUND/LITERATURE REVIEW

A substantial literature review was conducted prior to and throughout this study to appropriately define parameters for experimentation and continuously optimize device design and operation. The review was focused around three main topics of interest that are the basis of this study: photocatalysis using immobilized TNAs, photocatalysis combined with photoelectrocatalysis for the inactivation of bacteria using immobilized TNAs, and PC and PEC oxidation efficiency using immobilized TNAs in the presence of inorganic ions.

#### 2.1 Photocatalysis Using TiO<sub>2</sub> Nanotubes

Photocatalysis using TNAs has been a significant research focus in the fields of materials, chemical and metallurgical engineering, among others, over the last few decades. TiO<sub>2</sub> photocatalysis has been used for applications, such as water splitting, environmental pollutant remediation, wastewater treatment and air and water purification. Fujishima and Honda are viewed as pioneers in this field of research as they first discovered water splitting using irradiated TiO<sub>2</sub> as an electrode in 1972. Fox and Dulay thereafter found that irradiated semiconductors could catalyze reduction reactions of organic and inorganic compounds (Fox and Dulay 1993) and years later, Fujishima et al.

confirmed that many of these environmental pollutants could be completely mineralized (Fujishima 2007). Several studies have evaluated the photodegradation of textile dyes in wastewaters using  $\text{TiO}_2$  (Smith 2009, Zhou 2012, Liao 2012). Methyl orange (MO) is a common organic pollutant found in wastewater effluent in the textile industry, and thus, is commonly used as a model compound to determine PC activity. Several studies have demonstrated complete degradation of the dye in slurry reactors and reported relatively high efficiencies (Lachheb 2002, Gerischer 1995, Vautier 2001, Dijkstra 2001, Mehorta 2003).  $\text{TiO}_2$  nanotubes can be anodized on any titanium surface. Titanium foil, mesh and wires are the most common in this area of research.  $\text{TiO}_2$  is often times used as a powder as well. The disadvantage to using powders, or nanoparticles, is that posttreatment recovery of the catalyst can be inefficient and expensive (Dijkstra 2001). To overcome this inefficiency, immobilization of nanoparticles using commercially available Degussa P25 or  $\text{TiO}_2$  nanoparticles prepared using sol-gel methods has been carried out (Sayilkan 2007, Subramanian 2003, Carneiro 2004, Osugi 2005, Zanoni 2003). These methods, however, were shown to have a significantly reduced surface area and thereby increasing degradation times (Noorjahan 2003). Nie et al. (2013) reported that a  $\text{TiO}_2$  nanotubular photoanode exhibits increased inactivation rates over immobilized  $\text{TiO}_2$  nanoparticles under identical experimental conditions. Additionally, Kar et al. (2008) found that  $\text{TiO}_2$  nanotubes anodized on titanium wires showed a significant improvement in PC activity over nanotubes formed on foil when the conversion of a textile dye, MO, increased from 19% on foil to 40% on wires with identical nanotube dimensions illuminated over the same geometrical area (Kar et al., 2008).

## 2.2 Photocatalytic and Photoelectrocatalytic Inactivation of Bacteria

*E. coli* is a common type of bacteria analyzed in many bacterial inactivation studies. *E. coli* is commonly found in the lower intestine of warm-blooded organisms (Singleton 1999), but can also survive outside of the body, which make them an ideal indicator organism to test for fecal contamination (Feng 2002, Thompson 2007) and subsequently, a good model microorganism for experimental inactivation via PC and PEC in a laboratory controlled setting.

The PC inactivation of microorganisms using UV-irradiated TiO<sub>2</sub> is thought to have been discovered in 1988 when Matsunaga et al. (1988) first reported their work on the inactivation of *E. coli*. Using TiO<sub>2</sub> powders immobilized on acetylcellulose membranes, they discovered that low concentrations (10<sup>3</sup> colony forming units (CFU)/mL) of *E. coli* could be completely sterilized in 30 minutes under a mercury light intensity of 1100 microeinsteins/m<sup>2</sup> per s. They then concluded that increasing the light intensity as well as the amount of TiO<sub>2</sub> powders resulted in more rapid inactivation rates.

PEC bacterial inactivation has many distinct advantages over PC inactivation. Applying an external bias to the system produces ROSs such as, h<sup>+</sup>, •OH, O<sub>2</sub><sup>•-</sup>, and H<sub>2</sub>O<sub>2</sub>, etc. and also suppresses charge recombination, extending the lifetime of photoholes needed for direct inactivation. For effective PEC inactivation, a small voltage of ~1 V is sufficient for enhanced inactivation rates. The drawback to PEC inactivation lies in the reliance of available electricity.

Nie et al. (2014) conducted an extensive study comparing the efficiencies of PEC and PC inactivation of *E. coli* strains K-12 and its mutant *E. coli* BW25113 using a TiO<sub>2</sub>

nanotubular photoanode in a microfluidic device. The PEC and PC experiments were conducted in the same device irradiated with a constant UV light emitting diode array (365 nm) intensity of 28 mW/cm<sup>2</sup>; however, the PEC experiments included a constant applied external bias of 1.0 V. The results of the study concluded that PEC inactivation was more effective for both strains of *E. coli* than PC inactivation. They attributed the increased efficiency of PEC inactivation to the formation of additional h<sup>+</sup> reactive species during the process. This was determined by introducing different scavengers to remove specific ROSs in the system. When h<sup>+</sup> was removed from the system, a significant reduction in the bacterial inactivation rate was observed when compared to other scavengers. Scanning electron microscopy was employed to confirm cell death after PEC inactivation and demonstrated that cells were severely damaged and showed leakage of the intracellular components.

Baram et al. (2007) studied the enhancement of the photo-efficiency of electrochemically grown porous TiO<sub>2</sub> catalyst on foils and the inactivation rates of *E. coli* with applied voltages of up to 15 V. They found that increasing the applied potential to as much as 15 V in combination with UV light irradiation can drastically increase the bacterial inactivation rate as compared to 1 V with high *E. coli* concentrations (10<sup>6</sup>–10<sup>7</sup> CFU/mL). They stated that an anodic bias by itself has no influence on inactivation; rather, it causes water splitting only.



### 2.3 Photocatalytic and Photoelectrocatalytic Oxidation in the Presence of Inorganic Ions

Alrousan et al. (2009) studied the PC and photolytic inactivation rates of *E. coli* in surface water in the presence of nitrate and sulfate anions. Clean borosilicate glass sheets were dipcoated in a TiO<sub>2</sub>/methanol suspension for immobilization. The glass sheet was placed in a batch reactor as described by McMurray et al. (2004). Surface water was treated with membrane filtration prior to experimentation. In this setup, inactivation rates of *E. coli* were found to be significantly lower in surface water samples compared to distilled water. They cite a study conducted by Rincon and Pulgarin (2005) to explain their results. Rincon and Pulgarin (2005) suggest that organic compounds compete with bacteria for ROSs. They note that certain anions could adsorb onto the catalyst, inhibiting the PC inactivation efficiency. They also conclude that other constituents in surface water could absorb UV radiation reducing the effect of photolytic disinfection.

Nie et al. (2014) reported improved efficiencies in PEC inactivation efficiencies in the presence of NaCl and NaBr. They attribute this increase in efficiency to the formation of halide and dihalide radical anions during the inactivation process. They also found that no noticeable differences in inactivation efficiencies were observed in the presence of NaNO<sub>3</sub>, NaClO<sub>4</sub> and Na<sub>2</sub>SO<sub>4</sub>. It is believed that this is because they are only responsible for charge transport in a solution during PEC rather than acting as the reactants involved in the inactivation process.

## CHAPTER 3

### EXPERIMENTAL METHODS AND MATERIALS

#### 3.1 Device Fabrication

The batch reactor device contains a polycarbonate tube placed between sealed metal caps with port holes on either end. The anodically formed PC TNAs mesh was placed around the center of the device. The flow reactor contains PLA channels with a stainless steel backplate and a UV transparent polystyrene faceplate. The anodically formed PC TNAs wire was placed within the PLA channel, with a portion exposed to allow for connection to the power supply. The titanium mesh and wire (ESPI metals, 99.7 % Ti) were cut to size, ultrasonically cleaned in a 50/50 (by volume) methanol/isopropanol solution and then chemically polished in an acetic acid solution. Anodization was performed at 30 V for 60 m in a fluorinated ethylene glycol solution using mechanical stirring and a Pt gauze (52 mesh) cathode (Figure 2). After anodization, samples were rinsed with methanol and ultrasonicated in deionized water. The amorphously formed nanotubes were crystallized at 500 °C for 2 hours in a reducing atmosphere. The nanotubes used in the flow reactor were designed to incorporate a large overpotential, so that water splitting was not visually observed at 6 V on the TNA anode.

### 3.2 *E. coli* Preparation

*E. coli* W3110 was selected as the model bacteria to evaluate inactivation efficiencies under varying parameters and conditions. Bacterial strains were precultured in Luria Bertani (LB) broth at 40 °C for approximately 3 hours while shaking at 200 rpm. The culture was ready when the absorbance indicated the bacteria were near the peak of the logarithmic growth phase, or an absorbance of ~1.1 (OD<sub>600</sub>). The culture was diluted in the appropriate NaCl solution (10, 100, or 1000 ppm) until the desired cell density was achieved (between  $\sim 8.0 \times 10^3$  and  $\sim 1.0 \times 10^5$  CFU/mL), several orders of magnitude higher than those typically observed in natural waters ( $\sim 500$  CFU/100 mL).

### 3.3 *E. coli* Inactivation

Disinfection was conducted in the TNA containing batch reactor and flow reactors using a solar simulator with AM 1.5. Sunny days were simulated with 100 mW/cm<sup>2</sup> and cloudy day conditions were approximated by 25 mW/cm<sup>2</sup>. Incident UV irradiation on the surface of the flow reactor was typically  $\sim 1/10$ CFU of its respective full light spectrum intensity:  $\sim 3$  mW/cm<sup>2</sup> and  $\sim 10$  mW/cm<sup>2</sup> for 25 mW/cm<sup>2</sup> and 100 mW/cm<sup>2</sup>, respectively. The flow reactor combined photocatalysis with an applied anodic bias of up to 6 V.

#### *3.3.1 Batch Reactor Inactivation*

Contaminated water was manually pumped into the batch reactor with a 60 mL syringe. A schematic of the device is shown in Figure 3 and the experimental reactor is shown in Figure 4. Air continuously flowed through the solution to initiate aeration and

mixing. The TNA mesh was placed around the center of the reactor and irradiated with the aforementioned solar simulator. Samples were collected at varying times throughout the duration of the experiment for analysis via the plating method. Control experiments were performed using titanium mesh without the presence of TNAs.

### *3.3.2 Flow Reactor*

Contaminated water was gravity fed through the flow reactor at ~50 mL/m. A schematic of the device is shown in Figure 5 and the experimental setup is shown in Figure 6. For field assisted experiments, an anodic potential between 1 V and 6 V was applied to the TNA and a stainless steel plate was used as the cathode. A flow reactor was also tested with an aluminum anode to examine the effects of electroporation without a PC material. Control experiments were performed with the various anodes in the absence of UV irradiation. Additionally, blank devices without an anode material were also run as controls. Bacteria samples were well mixed before being poured through the device to avoid settling.

### 3.4 *E. coli* Analysis

The enumeration of *E. coli* concentrations before and after treatment was carried out by plating 50 µL aliquots onto LB agar. The LB agar plates were incubated overnight at 37 °C and colonies were visually identified and counted. Testing was performed in triplicate and an average of the results were taken as data points. Error bars are representative of the standard deviation between individual samples in each test. A paired t-test was performed to determine statistical significance at a 95% confidence level.

### 3.5 Natural Water Disinfection

Emigration Creek at Rotary Glen Park was used as a sample location for natural water disinfection as it represents a realistic source water from which one might drink while recreating in nature. Samples collected from this location were treated under natural sunlight using voltage conditions that were found to be favorable in the laboratory controlled *E. coli* experiments. In situ field data collected consisted of light intensity (total and UV), temperature, oxidation-reduction potential (ORP), conductivity and pH. The water was not turbid and contained little debris, so filtering was not performed. Sodium chloride was added to the system at concentrations of 10, 100 and 1000 ppm to simulate levels examined in the lab. Samples were brought to ChemTech-Ford Laboratories for enumeration of total coliform. Natural water samples were also brought back to the laboratory for testing under controlled sunlight and with the addition of NaCl. The sample water was filtered through a 0.2  $\mu\text{m}$  filter to ensure no bacteria remained in solution. Laboratory grade *E. coli* W3110 was then diluted into the natural water and run through the flow reactor device subjected to 100  $\text{mW}/\text{cm}^2$ . The test was also run with a spiked NaCl concentration of 100 ppm to examine the effects of additional chloride in the water and mimic previous laboratory experiments. After the gravity fed samples were treated at a flow rate of  $\sim 50$  mL/m, the samples were brought to ChemTech-Ford Laboratories for enumerated total coliform and *E. coli* analysis.

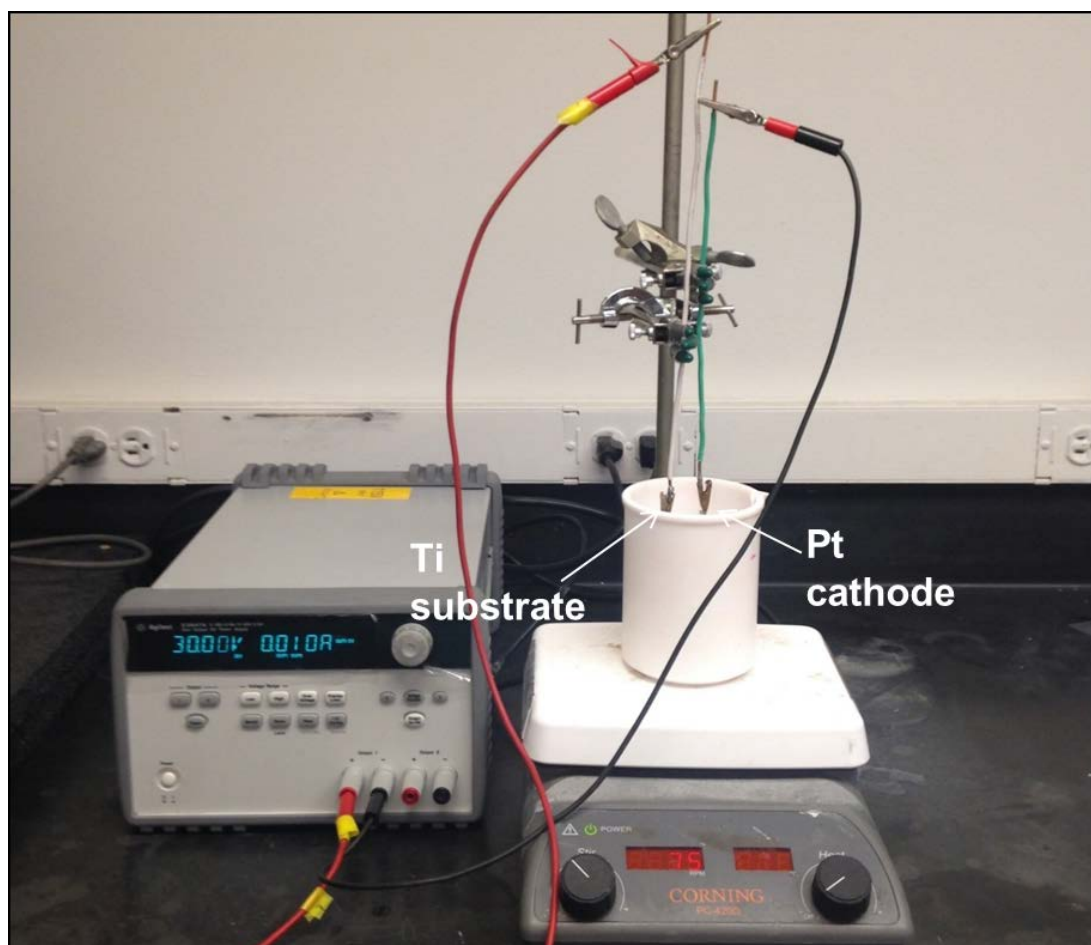


Figure 2. Synthesis setup for  $\text{TiO}_2$  fabrication..

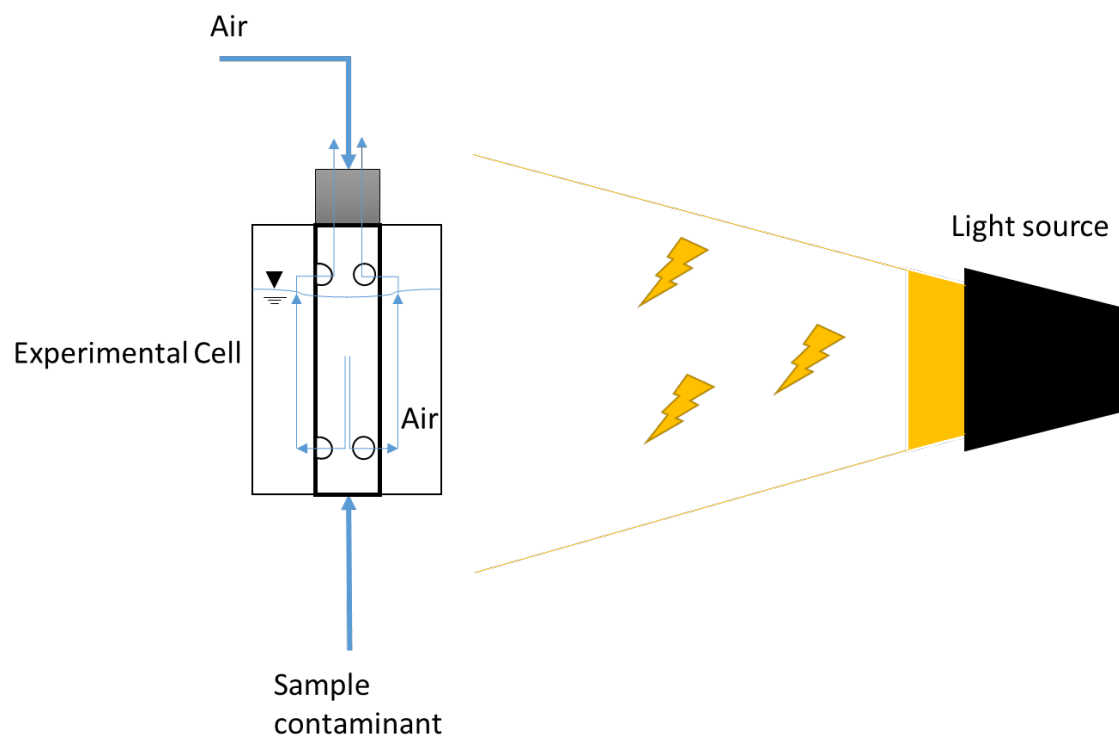


Figure 3. Schematic of the batch reactor device used for PC inactivation.





Figure 4. Batch reactor with TNA mesh. Mixing is achieved via aeration in the reactor.



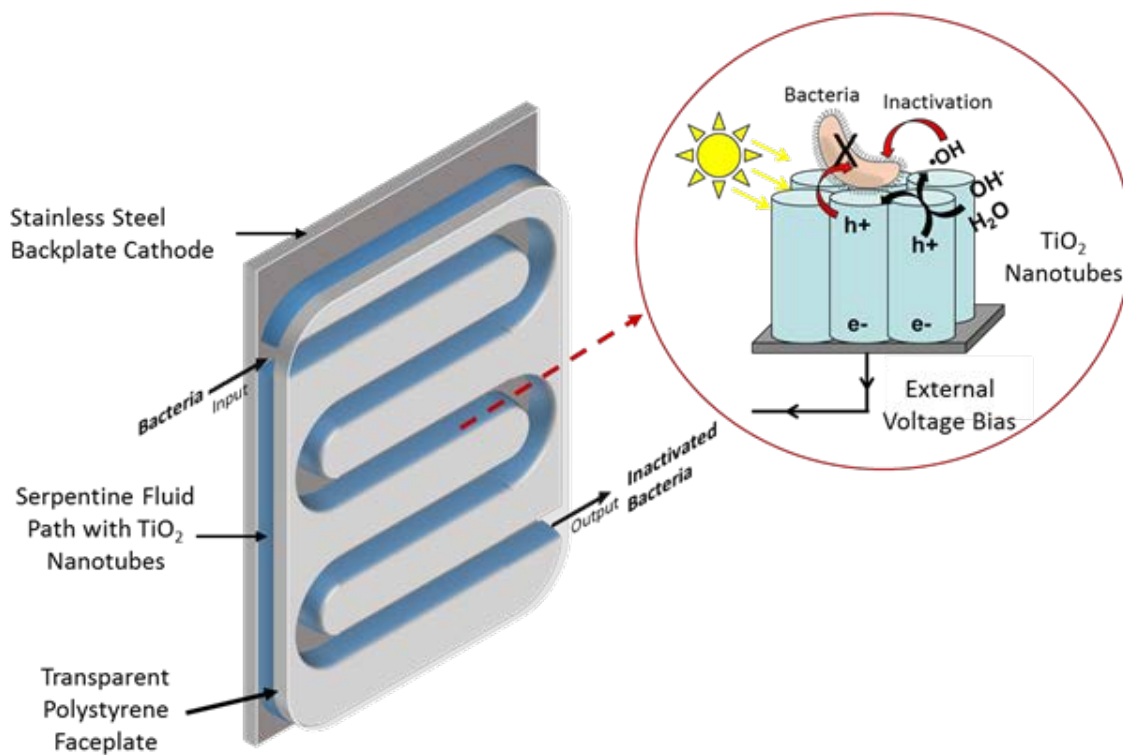


Figure 5. Schematic of the flow reactor used for photoelectrocatalytic inactivation.

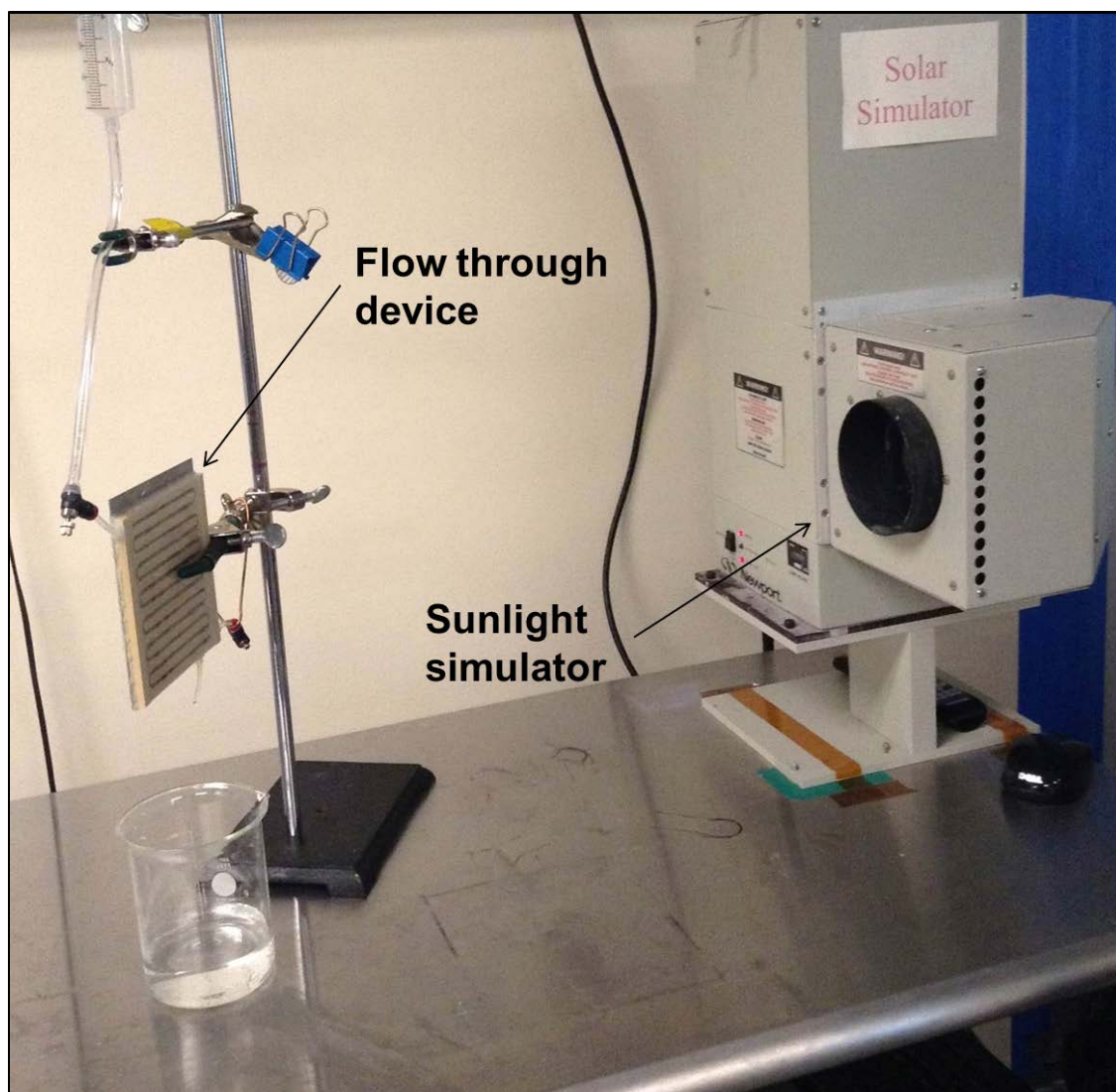


Figure 6. Setup used in the flow reactor experiments. Water is gravity fed through the device. The solar simulator provides natural light from 0-316  $\text{mW}/\text{cm}^2$ .

## CHAPTER 4

### RESULTS

#### 4.1 TNA Appearance

The TNA, shown in Figures 7 and 8, exhibited well defined tubes and/or nanograss, thin tubes that collapse and bundle when removed from the anodization solution. Average nanotube dimensions were 59 nm in diameter and 3.5  $\mu\text{m}$  in length.

#### 4.2 Inactivation Performance in a Polycarbonate Batch Reactor

Figure 9 shows the results of PC bacterial inactivation under identical experimental parameters with varying starting concentrations of *E. coli*. After 60 minutes the concentration of survived bacteria reduced by 10%, 60% and 90% for the high, medium and low starting concentrations, respectively, when compared to their control experiment (titanium wire). Each experiment displayed a reduction in active bacteria within the first 10 minutes, but the high and medium concentration experiments became relatively stable after the initial drop indicating poor inactivation rates over an extended period of time. The lower starting concentration (still several orders of magnitude higher than is typically found in natural surface waters) experiment continued to show a noticeable decline in survived bacteria through the entirety of the test.

### 4.3 Inactivation Performance in a Flow Reactor

The majority of the experiments that took place throughout the duration of this study were conducted in a flow reactor. The flow reactor exhibited improved inactivation performance and throughput over the batch reactor device. The remainder of this thesis focuses on the inactivation performance using a flow reactor under varying conditions.

#### *4.3.1 Inactivation Performance Under Simulated Conditions*

Inactivation results for different contact times within the reactor are shown in Figure 10. All tests were conducted with an irradiated intensity of  $100 \text{ mW/cm}^2$ . A contact time of 60 seconds under static conditions in the flow reactor showed a reduction of several hundred active bacteria between 0 V and 2 V, dropping to 479 CFU/mL at 2 V from the original concentration of 1010 CFU/mL, but no statistical difference between these applied voltages was seen. At 4 V, no bacteria were detected. A contact time of 15 seconds under dynamic conditions expressed a similar trend, but exhibiting higher values, about double of those observed for the 60 second treatment, dropping to 790 CFU/mL at 2 V with no statistical difference between 0 V and 2 V. At 3 V, no bacteria were detected. The blank devices run as controls exhibited no significant reduction or difference in active bacteria between experiments. Subsequent testing was conducted with a 15 second contact time under dynamic conditions, as this rate is closer to desirable product flow rates.

### *4.3.2 Inactivation Performance Under Different Irradiation*

#### *Conditions*

Reactor efficiency data under different irradiation conditions are shown in Figure 11. No statistical difference between the 0, 25 and 100 mW/cm<sup>2</sup> conditions was observed until 3 V, where bacteria concentrations dropped to 790, 210 and 20 CFU/mL, respectively.

### *4.3.3 Inactivation Performance with Different Anode Materials*

The difference between the TNA and the Al anode on bacterial inactivation is shown in Figure 12. Initially, the Al outperforms the TNA as ~70% bacterial inactivation is achieved. At 3 V, the TNA becomes drastically more effective, while the Al still does not show any statistical difference in its values. The Al anode consistently displays a significantly higher current than the TNA anode.

### *4.3.4 Inactivation Performance Under Different NaCl Loading*

#### *Conditions*

Inactivation with different NaCl concentration additions to the device are shown in Figure 13. A concentration of 10 ppm NaCl showed ~50% reduction at 1 V, but did not show a statistical difference in reduction between 1 V and 5 V. Little reduction in active bacteria was observed between 1 V and 2 V for the 100 ppm and 1000 ppm NaCl additions, but complete inactivation was achieved at 5 V and 4 V, respectively. Typical salt concentrations found in natural waters where experiments took place have been found to be approximately 50 ppm.

#### *4.3.5 Inactivation Performance Under Natural and Simulated*

##### *Sunlight Conditions*

Chemical analysis of the water collected at Emigration Creek is shown in Table 2. Experiments similar to those run in the laboratory were conducted under natural conditions at Emigration Creek. Table 3 and Table 4 show the results of the experiments conducted under the conditions listed in Table 2. Total coliform were enumerated as CFU/100 mL. Total coliform was shown to reduce from a starting concentration of 2300 CFU/100 mL to 52 CFU/100 mL at 6 V and with a spiked concentration of 100 ppm NaCl. The results from experiments conducted in the laboratory with natural water samples are shown in Table 4. Complete inactivation was observed from an initial concentration of 2100 CFU/100 mL using an applied bias of 6 V.

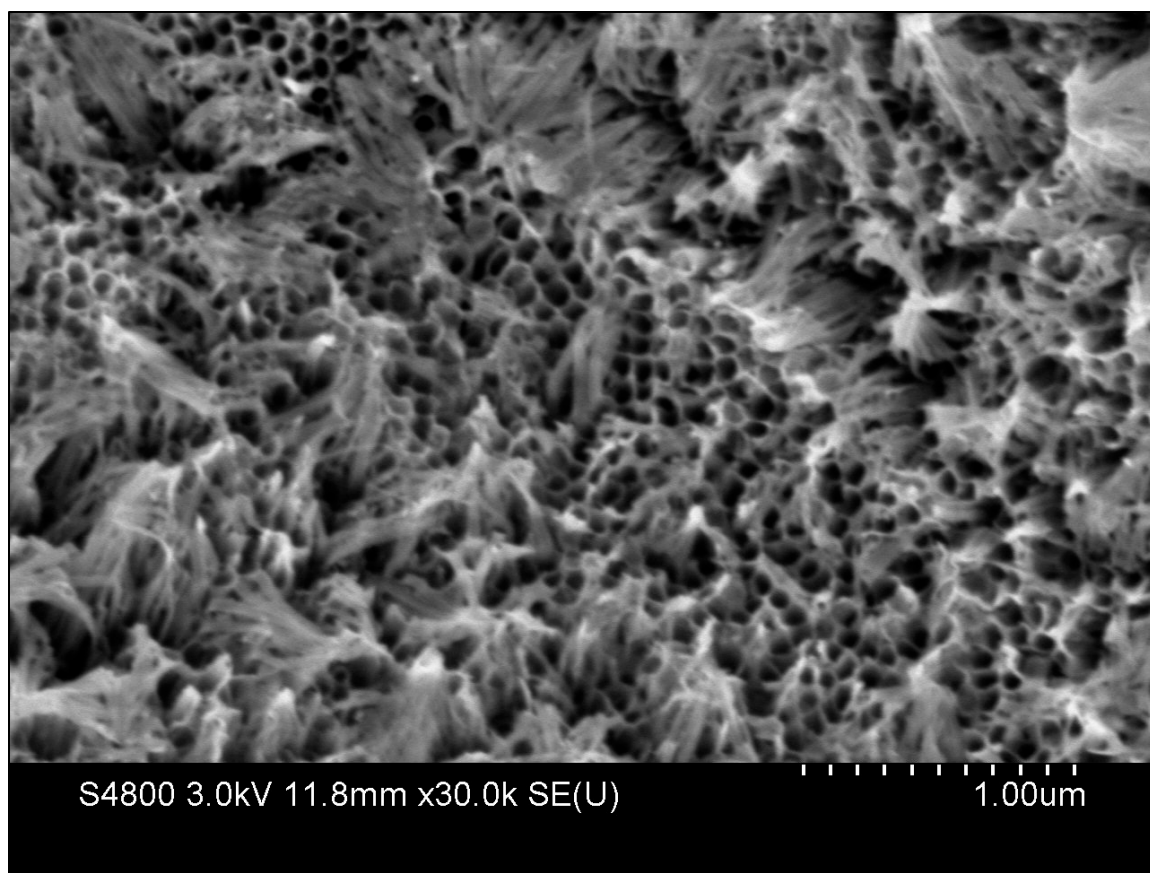


Figure 7. Top view SEM image of nanotubes annealed in nitrogen/2% hydrogen blend on the titanium wire used in the flow reactor experiments.

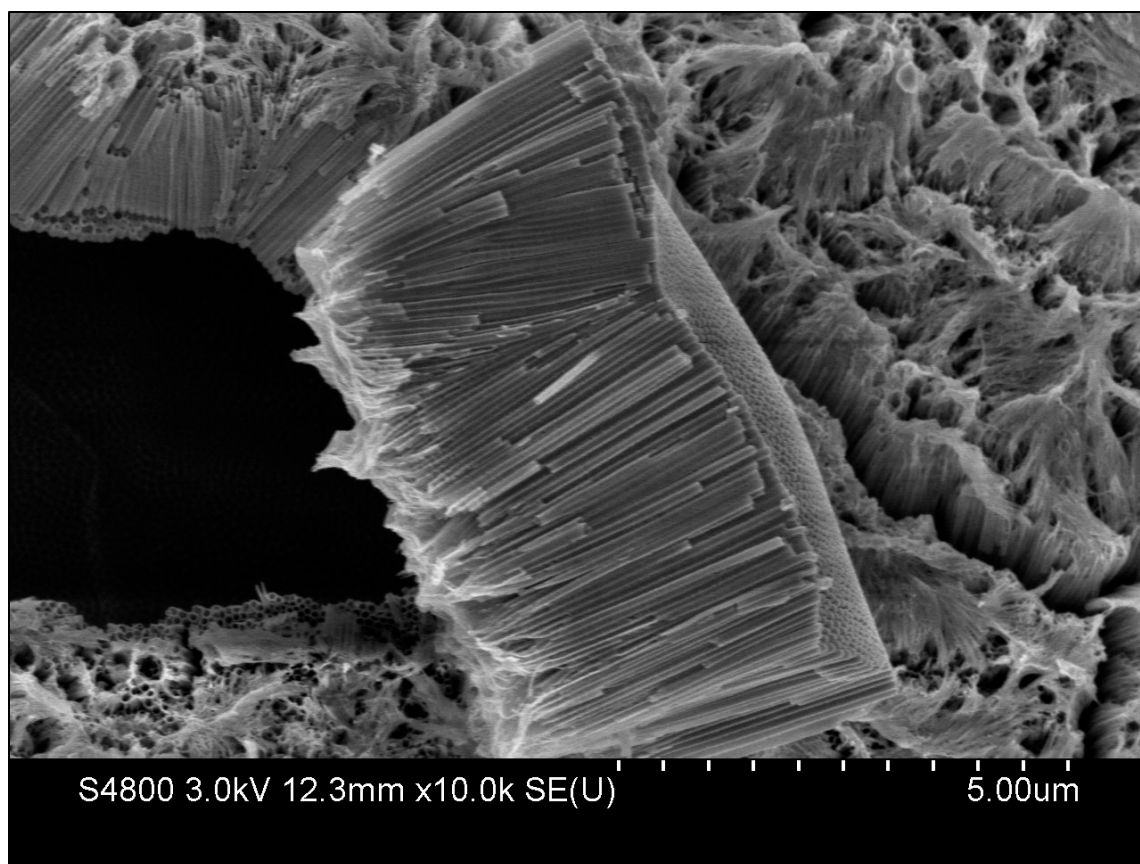


Figure 8. Side view SEM image of nanotubes annealed in a nitrogen/2% hydrogen blend on the titanium wire used in the flow reactor device experiments.



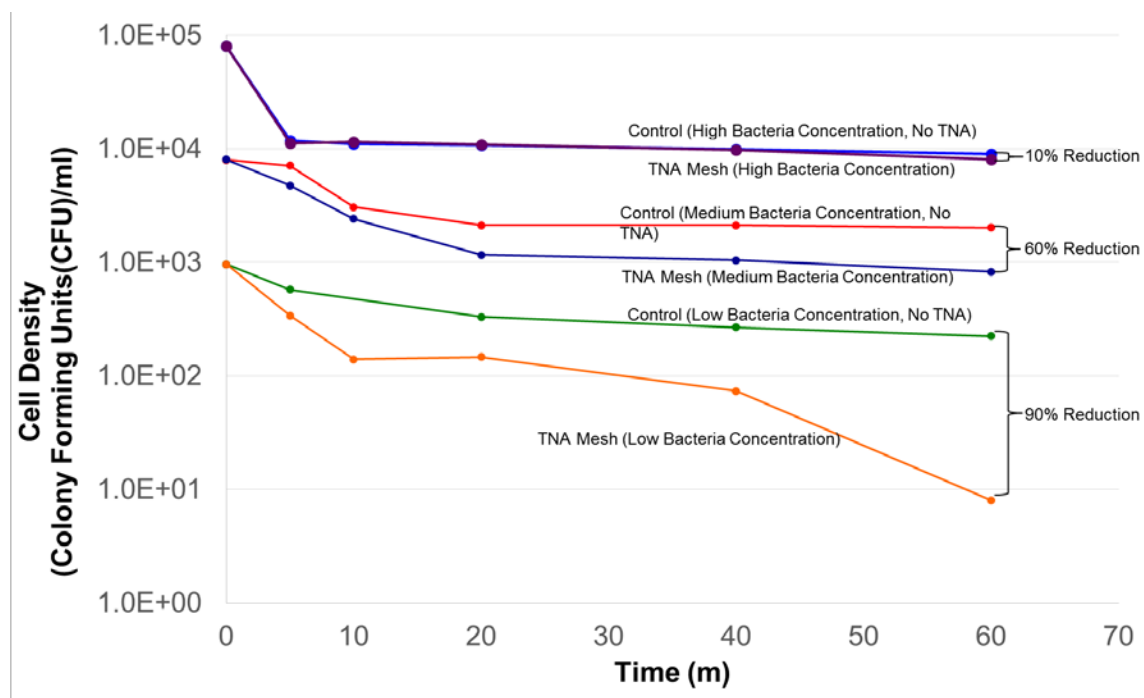


Figure 9. Batch reactor experiments with irradiation at 100 mW/cm<sup>2</sup>.

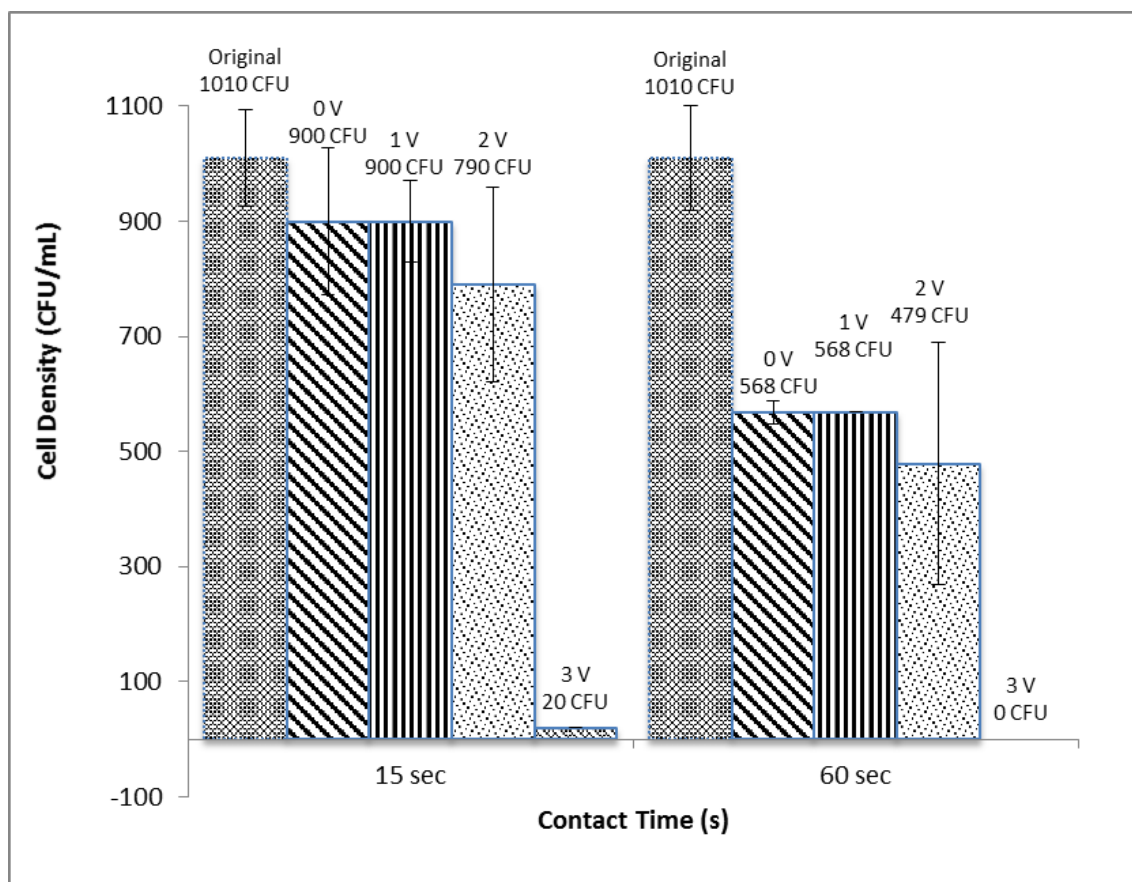


Figure 10. Bacterial inactivation performance under 15 second and 60 second contact times subjected to 100 mW/cm<sup>2</sup> in the flow-through device. The active bacteria concentration decreases at low voltages for each time of contact, but more significantly with a 60 second contact time.

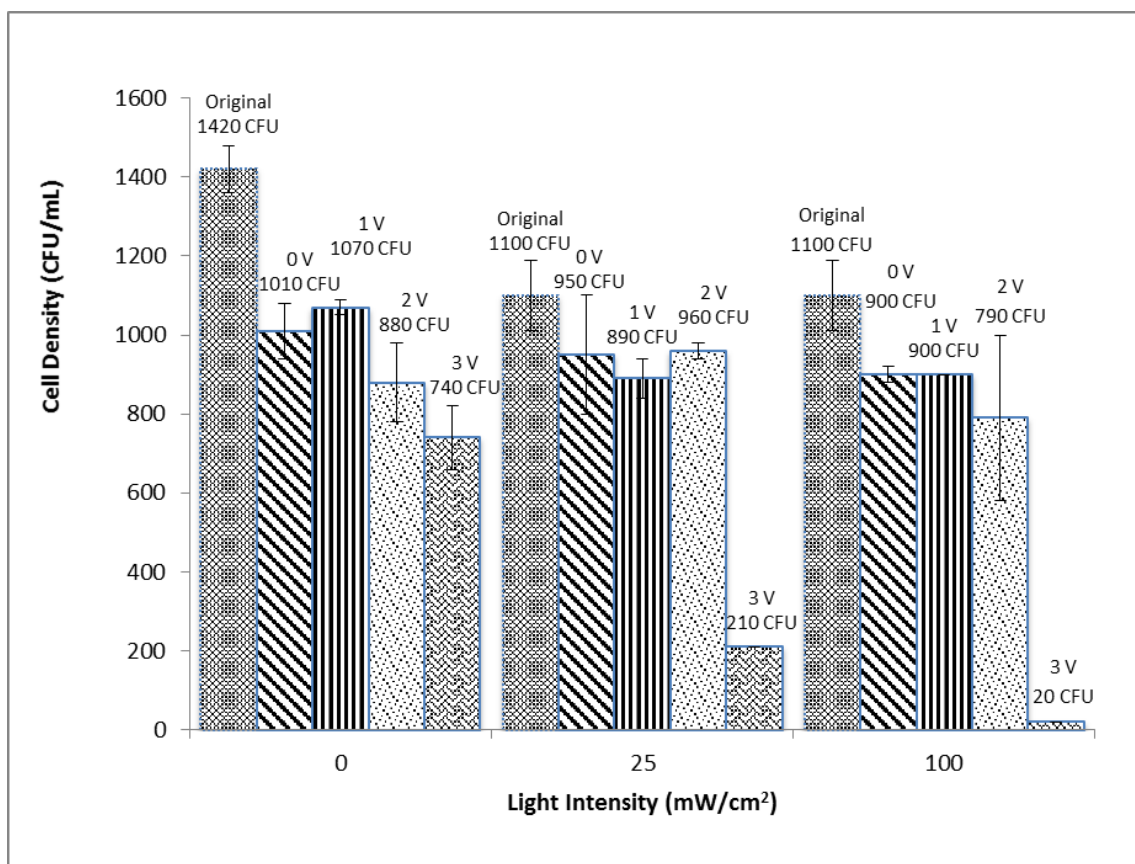


Figure 11. Bacterial inactivation performance under simulated conditions for 0 mW/cm<sup>2</sup>, 25 mW/cm<sup>2</sup>, and 100 mW/cm<sup>2</sup> showing the effect that different levels of inactivation have on the system. Bacteria subjected to 3 V and 25 mW/cm<sup>2</sup> exhibited ~80% inactivation, whereas bacteria subjected to 3 V and 100 mW/cm<sup>2</sup> exhibited ~98% inactivation.

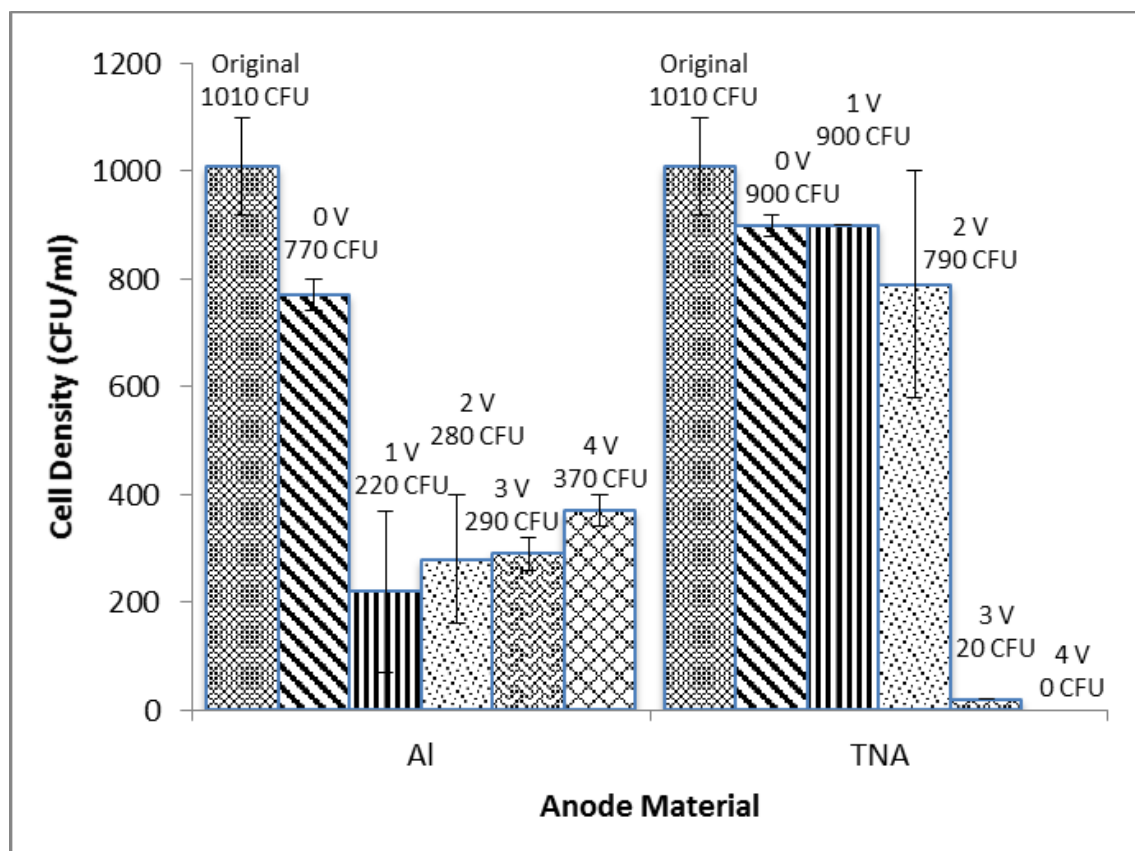


Figure 12. Bacterial inactivation performance using Al and TNA anode materials. The Al anode showed a drastic decrease in active bacteria at a low voltage, but was unable to completely inactivate all bacteria while the TNA anode expressed a small decrease in active bacteria at a lower voltage, but was able to achieve complete inactivation with increased voltage.

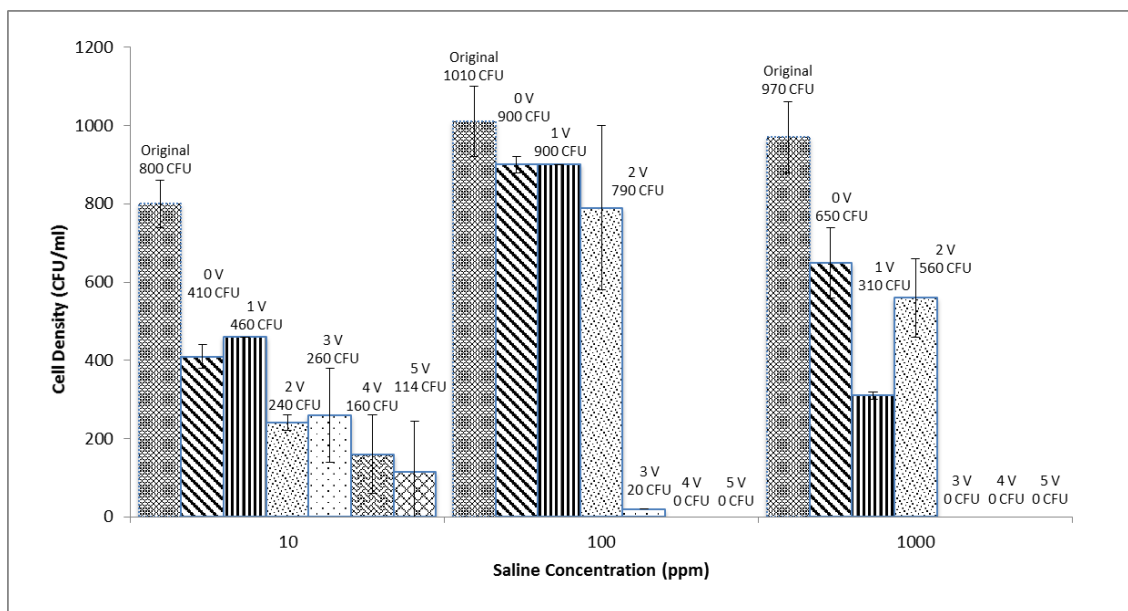


Figure 13. Bacterial inactivation performance using different NaCl concentrations under 100 mW/cm<sup>2</sup> irradiation. Bacterial inactivation became more effective with higher concentrations of NaCl.

Table 2. Environmental and water conditions and chemistry in Emigration Creek at Rotary Glen Park.

Parameter	
Flow Rate	50 mL/min
Light Intensity	100 mW/cm <sup>2</sup>
UV	12.6 mW/cm <sup>2</sup>
pH	8.02
Conductivity	1186 µS
ORP	397 mV
Temperature	12.2°C
Sulfate	152 ppm
Nitrate	0.4 ppm
Nitrite	<0.1 ppm
Chloride	1 ppm

Table 3. Biocide results, within 10% error, from device testing Emigration Creek water under natural settings.

<b>Condition</b>	<b>Total Coliform (CFU/100 mL)</b>
Original	2300
0 V, 0 ppm NaCl	>2400
0 V, 10 ppm	>2400
0 V, 100 ppm	>2400
4 V, 0 ppm NaCl	1100
4 V, 10 ppm NaCl	1300
4 V, 100 ppm NaCl	300
5 V, 0 ppm NaCl	1000
5 V, 10 ppm NaCl	400
5 V, 100 ppm	650
6 V, 0 ppm NaCl	490
6 V, 10 ppm	50
6 V, 100 ppm	52

Table 4. Biocide results, within 10% error, from device testing Emigration Creek water under simulated solar irradiation of 100mW/cm<sup>2</sup>.

<b>Condition</b>	<b>Total Coliform (CFU/100 mL)</b>
Original	2100
Blank	2600
4 V	1700
6 V	0

## CHAPTER 5

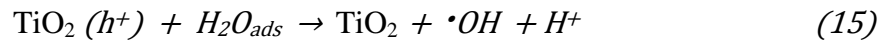
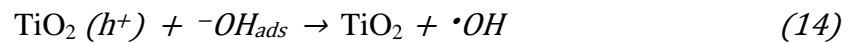
### DISCUSSION

#### 5.1 Inactivation Mechanism

The environment inside the reactors during treatment is unfavorable for pathogens due to both PC generation of radicals and the applied electric field. Irradiation of the TNA with light  $<387$  nm causes bound electrons to excite into the conduction band, leaving behind a hole situated in the valence band, Eq. 13.

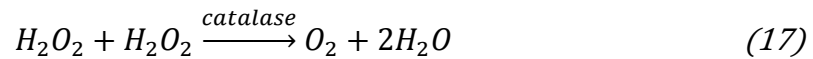
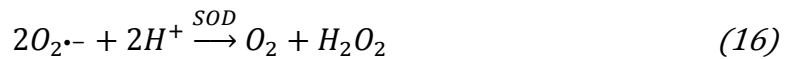


These holes are then free to react with adsorbed  $^-OH$  and  $H_2O$ , generating  $\bullet OH$ . The reactions, summarized in Eqs. 14 and 15, are theorized to be of great importance in biocide, as  $\bullet OH$  has the highest oxidation power of aqueous and elemental radical species that can be generated during PC (Nie 2014, Munter 2001).



During PEC, electrons are driven into the circuit via the nanotubes and titanium substrate to reduce their recombination rate with holes. This extended time period allows holes to directly participate in the oxidation reaction with the bacteria, which is especially important as holes have a higher relative oxidation power than  $\bullet\text{OH}$  (Munter 2001). Figure 1 shows a depiction of the oxidation process through direct ( $h^+(\text{VB})$ ) and indirect processes (i.e.,  $\bullet\text{OH}$ ).

However, from the data collected, it was observed that PC and PEC (<2 V) alone does not inactivate the bacteria at flow rates that are necessary for this type of device. Gram-negative bacteria, such as *E. coli*, produce the enzyme superoxide dismutase (SOD) in response to oxidative stress. This enzyme can transform radicals into hydrogen peroxide ( $\text{H}_2\text{O}_2$ ) and molecular oxygen via reactions Eq. 16. Bacteria then produce catalase which breaks down intracellular  $\text{H}_2\text{O}_2$  into water and oxygen (Eq. 17) (Rincon 2003).



## 5.2 Electroporation

To make the device more effective without increasing the overall size or contact time with the TNA, a voltage above what is required for PEC (<2 V) was applied to the system to induce electroporation. In electroporation, high voltage electric fields temporarily destabilize the lipid bilayer and proteins composing the cell membrane



(United States Food and Drug Administration 2011). This reversible breakdown results in permeation of the cell membrane and unregulated permeation of molecules. Pore size is a function of electric field intensity and duration within the field. Field strength for reversible breakdown is in the range of 3 – 24 kV/cm for bacteria cells (Mernier 2012, BTX Harvard Apparatus 2015). Long time periods at these field strengths and/or fields above this range can lead to irreversible mechanical destruction of the membrane.

In pulsed electric field systems, pulses of high voltage reach between 20–80 kV/cm (United States Food and Drug Administration 2011). These complex and energy intensive systems are not feasible for portable device operation; however, as the device described in this paper does not rely solely on electric fields for cell lysing, the power requirements can be substantially reduced. At 4 V, the device is calculated to have an electric field of ~0.08 kV/cm. Although this field strength is below field strengths reported for bacterial electroporation (~2.2 kV/cm) (United States Food and Drug Administration 2011), it is proposed that just enough permeation is occurring to allow radical penetration into the cell. This is likely attributed to the increased time (15 seconds) in which the bacteria is exposed to high voltage for electroporation, as typical electroporation is conducted within a fraction of a second. This has been reported by other researchers when using electroporation in microdevices (less than 2 V continuous DC) (Guido 2012). Complete inactivation can occur at low field strengths as radicals directly attack cell components without having to oxidize the cell defense enzymes or break down the membrane. Increasing the irradiation intensity on the system shows little effect at <3 V as the channels are too wide and the flow is too fast for PC generated radicals to be effective on their own. However, at 3 V, enough photogenerated radicals

are present to significantly increase the rate of disinfection. After an initial drop in cell density, the Al anode maintained inactivation levels between 1 V and 4 V. However, the PC material plays an important role in the disinfection process as the TNA generates electron hole pairs, while the Al anode does not.

### 5.3 Ion Effect on Disinfection

Increasing the chloride concentration was observed to require a decrease in the voltage at which inactivation was observed. These results agreed with Nie et al., who reported that chloride and dihalide ions increase bioactivity in PEC as the photogenerated holes now have a longer lifetime and can ionize chlorine through the following reactions (Eqs. 18 and 19) (Nie 2014):



Alrousan et al. found that the photolytic disinfection rate was slightly reduced when sulfate and nitrate ions were present in solution when a TiO<sub>2</sub> film was used. Sulfates were reported to block active sites via adsorption to TiO<sub>2</sub> surfaces (Alrousan 2009), while nitrates absorb UV light. The drop in current with time for the natural water is thought to be caused by the deposition of sulfates on the TiO<sub>2</sub> surface. The simulated sunlight experiments are thought to have been more efficient than the natural sunlight experiments due to the columnated light concentrated directly on the surface of the

disinfection device. Ongoing research is addressing these challenges through device optimization to overcome the reduction in inactivation rates for natural waters.

#### 5.4 Combined PC and PEC

Inactivation of *E. coli* in a flow reactor device using a combination of photocatalysis and electroporation occurred in both simulated and natural water. A higher voltage was needed in the natural water containing additional inorganic and organic ions. For each of the parameters evaluated, field assisted PC was more effective for bacterial inactivation than PC alone. The optimal applied bias for complete inactivation was  $>3$  V. Increasing the NaCl concentration in solution improved the efficiency of the device, but should be limited to 250 ppm, as this is below the Environmental Protection Agency Secondary Drinking Water Regulations for chlorides in drinking water (United States Environmental Protection Agency 2014). The implications of this technology advances the understanding of the combination of electroporation with PEC and PC oxidation of harmful constituents in surface water and could lead to more cost effective water treatment methods that could eventually replace traditional methods.

## CHAPTER 6

### CONCLUSIONS

#### 6.1 Analysis Results

The results of this study show the potential for using immobilized TNAs as a cost effective method for disinfecting contaminated surface waters. Each reactor used exhibited promising inactivation efficiencies for a real world water disinfection device for POU purposes. The PC batch reactor was able to reduce the amount of survived *E. coli* by 90% in 60 minutes and the flow reactor exhibited increased inactivation rates with the application of a small anodic bias. The combination of photocatalysis and an applied external anodic bias in the flow reactor reported to completely inactivate higher levels of bacteria than are typically found in natural surface water with a throughput rate of 50 mL/m. Reducing the flow in the reactor, and therefore increasing the contact time, exhibited more efficient inactivation rates between 0 and 3 V with complete inactivation at 3 V and 60 seconds in the reactor. Although irradiation intensity is necessary for radical formation and direct oxidation, no statistical difference was observed in the reactor with increasing irradiation intensities until 3 V was applied. Testing the flow reactor with an Al anode alongside a TNA anode expressed the importance of the TNAs for bacterial inactivation by achieving complete inactivation at 4 V with the TNA anode, whereas the Al anode was unable to inactivate the bacteria at 4 V. The addition of NaCl

concentrations in the contaminated samples resulted in improved inactivation rates with increasing concentrations, which can be attributed to the addition of dihalide ions in solution contributing to the oxidation process. Finally, the natural water samples presented difficulty for complete bacterial inactivation. This was likely due to the addition of organic and inorganic ions and other constituents found in nature that possibly block the active sites and/or absorbing of UV light; however, a significant reduction in survived bacteria was still observed with a higher applied bias of 6 V under natural conditions. These results express the feasibility of the proposed technology for real world applications. Certainly, this technology should be further developed and optimized to treat all types of surface water under a worst-case scenario prior to commercialization for human use. The device used in this study would be ideal as a portable POU water disinfection unit for outdoor enthusiasts or in emergency situations. It is also believed that this system could be scaled up to be used for larger applications such as residential water treatment for primary drinking or secondary water uses. The incorporation of batteries or a portable solar panel on a flow reactor disinfection device such as the one in this study could allow a user to more efficiently disinfect contaminated water.

## 6.2 Future Research

The research conducted for this study, albeit comprehensive, requires a much more inclusive assessment to develop a portable POU water disinfection system for human use. This study merely scratches the surface of the fundamentals for using TNAs for the PC inactivation of water-borne pathogens in a POU water disinfection device. To gain a fully comprehensive understanding of this potential technology, future studies

should focus on the variations of water chemistries found in surface waters, the effects that varying levels of turbidity have on the device and the effectiveness of the device for treating a wide array of other pathogens such as giardia, cryptosporidium and viruses. Further, a deeper understanding of the specific disinfection mechanism also needs to be understood. Ongoing research on the effects of common ions in surface waters, specifically chlorides, nitrates and sulfates is currently underway. Additionally, laboratory experiments are focused on bacterial inactivation in the aforementioned flow reactor without the presence of light so disinfection can take place without a dependence on available sunlight. Future experiments will be conducted introducing scavengers to remove ROSs to determine which ROSs are responsible for bacterial inactivation so that device optimization can be further improved.

## LITERATURE CITED

- Alrousan, D., Dunlop, P., McMurray, T., Byrne, J., 2009. Photocatalytic inactivation of *E. coli* in surface water using immobilized nanoparticle TiO<sub>2</sub> films. *Wat. Res.*, *43*, 47–54.
- ASCE, 2013. 2013 Report Card for America's Infrastructure. Accessed online: <http://www.infrastructurereportcard.org/a/#p/drinking-water/conditions-and-capacity>
- Baram, N., Starosvetsky, D., Starovetsky, J., Ephshtein, M., Armon, R., Ein-Eli, Y., 2011. Photocatalytic inactivation of microorganisms using nanotubular TiO<sub>2</sub>. *Appl. Catal. B.*, *101*:212–219.
- BTX Harvard Apparatus: Electroporation Applications, 2015. Accessed online: <http://www.btxonline.com/electroporation-1/>
- Butterfield, I., Christensen, P., Curtis, T., Gunlazuardi, J., 1997. Water disinfection using an immobilized titanium dioxide film in a photochemical reactor with electric field enhancement. *Wat. Res.*, *31*, 675–677.
- Carneiro, P. A., Osugi, M. E., Sene, J. J., Anderson, M. A., Zanoni, M. V. B., 2004. Evaluation of color removal and degradation of a reactive textile azo dye on nanoporous TiO<sub>2</sub> thin-film electrodes. *Electrochim. Acta*, *49*, 3807–3820.
- Cheng, Y. W., Chan, R. C. Y., Wong, P. K., 2007. Disinfection of *Legionella pneumophila* by photocatalytic oxidation. *Wat. Res.*, *41*, 842–852.
- Cho, M., Chung, H., Choi, W., Yoon, J., 2004. Linear correlation between inactivation of *E. coli* and OH radical concentration in TiO<sub>2</sub> photocatalytic disinfection. *Wat. Res.*, *38*, 1069–1077.
- Chong, M. N., Jin, B., Chow, C. W. K., Saint, C., 2010. Recent developments in photocatalytic water treatment technology: a review. *Wat. Res.*, *44*, 2997.
- Dalrymple, O.K., Stefanakos, E., Trotz, M.A., Goswami, D. Y., 2010. A review of the mechanisms and modeling of photocatalytic disinfection. *Appl. Catal. B: Environ.*, *98*, 27–38.

- Dijkstra, M. F. J., Michorius, A., Buwalda, H., Panneman, H. J., Winkelman, J. G. M., Beenackers, A. A. C. M., 2001. Comparison of the efficiency of immobilized and suspended systems in photocatalytic degradation. *Catal. Today*, 66, 487–494
- Feng, P., Weagant, S., Grant, M., 2002. Enumeration of *Escherichia coli* and the coliform bacteria. Bacteriological Analytical Manual (8<sup>th</sup> ed). FDA/Center for Food Safety & Applied Nutrition.
- Foster, H. A., Ditta, I. B., Varghese, S., Steele, A., 2011. Photocatalytic disinfection using titanium dioxide: spectrum and mechanism of antimicrobial activity. *Appl. Microbiol. Biotechnol.* 90, 1847–1868.
- Fox, M., & Dulay, M., 1993. Heterogeneous photocatalysis. *Chemical Reviews*, 93, pp. 341–357.
- Fujishima, A and Honda, K, 1972. Electrochemical photolysis of water at a semiconductor electrode. *Nature*, 238, 37.
- Fujishima, A., Zhang, X., & Tryk, D., 2007. Heterogeneous photocatalysis: from water photocatalysis to applications in environmental cleanup. *International Journal of Hydrogen Energy*, 32, pp. 2664–2672.
- Gerischer, H., 1993. Photoelectrochemical catalysis of the oxidation of organic molecules by oxygen on small semiconductor particles with TiO<sub>2</sub> as an example. *Electrochim. Acta.*, 38, 3-9.
- Gerischer, H., 1995. Photocatalysis in aqueous-solution with small TiO<sub>2</sub> particles and the dependence of the quantum yield on particle-size and light-intensity. *Electrochim. Acta*, 40, 1277–1281.
- Guido, I., Xiong, C., Fang, J., 2012. Low-voltage electroporation with fluidic microelectrodes. *Microelectronic Engineering*, 98 (0), 707-710.
- Kar, A., Smith, Y., Subramanian, V., 2009. Improved photocatalytic degradation of textile dye using titanium dioxide nanotubes formed over titanium wires. *Environ. Sci. Technol.*, 43, 3260–3265.
- Kim, S., Ghafoor, K., Lee, J., Feng, M., Hong, J., Lee, D., Park, J., 2013. Bacterial inactivation in water, DNA strand breaking, and membrane damage induced by ultraviolet-assisted titanium dioxide photocatalysis. *Wat. Res.*, 47, 4403-4411.
- Lachheb, H., Puzenat, E., Houas, A., Ksibi, M., Elaloui, E., Guillard, C., Herrmann, J. M., 2002. Photocatalytic degradation of various types of dyes (alizarin S; crocein orange G; methyl red; congo red; methylene blue) in water by UV-irradiated titania. *Appl. Catal., B*, 39, 17590.



- Legrini, O., Oliveros, E. & Braun, A.M., 1993. Photochemical processes for water treatment. *Chemical Reviews*, 93, pp. 671–698.
- Liao, J., Lin, S., Zhang, L., Pan, N., Cao, X., Li, J., 2011. Photocatalytic degradation of methyl orange using a TiO<sub>2</sub>/Ti mesh electrode with 3D nanotube arrays. *Appl. Mater. Interfaces*, 4, 171–177.
- Linsebigler, A., Lu, G., & Yates, J., 1995. Photocatalysis on surfaces: principles, mechanisms, and selected results. *Chemical Reviews*, 95, pp. 735–758.
- Lu, A. X., Zhou, L., Z.L. Zhang, Z. L., Shi, W. L., Xie, Z. X., Xie, H. Y., Pang, D. W., Shen, P., 2003. Cell damage induced by photocatalysis of TiO<sub>2</sub> thin films. *Langmuir*, 19, 8765–8768.
- Markowska-Szczupak, A., Ulfig, K., Morawski, A. W., 2011. The application of titanium dioxide for deactivation of bioparticulates: an overview. *Catal. Today*, 169, 249–257.
- Matsunaga, T., Okochi, M., 1995. TiO<sub>2</sub>-mediated photochemical disinfection of *Escherichia coli* using optical fibers. *Environ. Sci. Technol.*, 29, 501-505.
- Matsunaga, T., Tomoda, R., Nakajima, T., Wake, H., 1985. Photoelectrochemical sterilization of microbial cells by semi-conductor powders. *FEMS Microbiol. Lett.*, 29 (211-214).
- Matsunaga, T., Tomoda, R., Nakajima, Y., Nakamura, N., and Komine, T., 1988. Continuous-sterilization system that uses photosemiconductor powders. *Appl. Environ. Microbio.*, 54, 1330–1333.
- Mehrotra, K., Yablonsky, G. S., Ray, A. K., 2003. Kinetic studies of photocatalytic degradation in a TiO<sub>2</sub> slurry system: distinguishing working regimes and determining rate dependences. *Ind. Eng. Chem. Res.*, 42, 2273–2281.
- Mernier, G., Martinez-Duarte, R., Lehal, R., Radtke, F., Renaud, P., 2012. Very high throughput electrical cell lysis and extraction of intracellular compounds using 3D carbon electrodes in lab-on-a-chip devices. *Micromachines*, 3, 574-581.
- Munter, R., 2001. Advanced oxidation processes - current status and prospects. *Proc. Estonian Acad. Sci. Chem.*, 50, 59-80.
- Nie, X., Li, G., Gao, M., Sun, H., Liu, X., Zhao, H., Wong, P., An, T., 2014. Comparative study on the photoelectrocatalytic inactivation of *Escherichia coli* K12 and its mutant *Escherichia coli* BW25113 using TiO<sub>2</sub> nanotubes as a photoanode. *Appl. Catal. B-Environ.*, 147, 562–570.

- Noorjahan, M., Reddy, M. P., Kumari, V. D., Lavedrine, B., Boule, P., Subrahmanyam, M., 2003. Photocatalytic degradation of H-acid over a novel TiO<sub>2</sub> thin film fixed bed reactor and in aqueous suspensions. *J. Photochem. Photobiol. A*, 156, 179–187.
- Osugi, M. E., Umbuzeiro, G. A., Anderson, M. A., Zanoni, M. V. B., 2005. Degradation of metallophthalocyanine dye by combined processes of electrochemistry and photoelectrochemistry. *Electrochim. Acta*, 50, 5261–5269.
- Outdoor Industry Association, 2014. The outdoor recreation economy. Accessed online: <http://outdoorindustry.org/advocacy/recreation/economy.html>
- Pelaez, M., Nolan, N., Pillai, S., Seery, M., Falaras, P., Krontos, A., Dunlop, P., Hamilton, J., Byrne, J., O'Shea, K., Entezari, M., Dionysiou, D., 2012. A review on the visible light active titanium dioxide photocatalysts for environmental applications. *Appl. Catal. B-Environ.*, 125, 331–349.
- Pruss-Ustun, A., Bartram, J., Clasen, T., Colford Jr, J., Cumming, O., Curtis, V., Bonjour, S., Dangour, A., De France, J., Fewtrell, L., Freeman, M., Gordon, B., Hunter, P., Johnston, R., Mathers, C., Mausezahl, D., Medlicott, K., Neira, M., Stocks, M., Wolf, J., Cairncross, S., 2014. Burden of disease from inadequate water, sanitation and hygiene in low- and middle-income settings: a retrospective analysis of data from 145 countries. *Tropical Medicine and International Health*, 19, 894–905.
- Rincon, A., Pulgarin, C., 2003. Photocatalytic inactivation of *E. coli*: effect of (continuous-intermittent) light intensity and of (suspended-fixed) TiO<sub>2</sub> concentration. *Appl. Catal. B-Environ.*, 44, 263–284.
- Saravanan, P., Pakshirajan, K., & Saha, P., 2009. Degradation of phenol by TiO<sub>2</sub>-based heterogeneous photocatalysts in presence of sunlight. *Journal of Hydro-environment Research*, 3, pp. 45–50.
- Sayilkan, H., 2007. Improved photocatalytic activity of Sn 4 (+)-doped and undoped TiO<sub>2</sub> thin film coated stainless steel under UV and visible irradiation. *Appl. Catal.*, A, 319, 230–236.
- Singleton, P. 1999. Bacteria in Biology. Biotechnology and Medicine (5<sup>th</sup> ed). Wiley. Pp. 444-454. ISBN 0-471-98880-4.
- Smith, Y. R., Kar, A., Subramanian, V., 2009. Investigation of physicochemical parameters that influence photocatalytic degradation of methyl orange over TiO<sub>2</sub> nanotubes. *Ind. Eng. Chem. Res.*, 48, 10268–10276.

- Smith, Y., Ray, R., Carlson, K., Sarma, B., Misra, M., 2013. Self-ordered titanium dioxide nanotube arrays: anodic synthesis and their photo/electro-catalytic applications. *Materials*, 6, 2892-2957.
- Subramanian, V., Kamat, P. V., Wolf, E. E., 2003. Mass-transfer and kinetic studies during the photocatalytic degradation of an azo dye on optically transparent electrode thin film. *Ind. Eng. Chem. Res.*, 42, 2131–2138.
- Sunada, K., Watanabe, T., Hashimoto, K., 2003. Bactericidal activity of copper-deposited TiO<sub>2</sub> film under weak UV light illumination. *Environ. Sci. Technol.*, 37, 4785-4789.
- Thompson, A., 2007. *E. coli* Thrives in Beach Sands. Accessed online: <http://www.livescience.com/4492-coli-thrives-beach-sands.html>.
- United Nations Water, 2013. International Year of Water Cooperation. Accessed online: <http://www.unwater.org/water-cooperation-2013/water-cooperation/facts-and-figures/en/0>
- United States Environmental Protection Agency, 2013. Secondary Drinking Water Regulations: Guidance for Nuisance Chemicals. Accessed online: <http://water.epa.gov/drink/contaminants/secondarystandards.cfm>
- United States Food and Drug Administration, 2011. Kinetics of Microbial Inactivation for Alternative Food Processing Technologies -- Pulsed Electric Fields. Accessed online: <http://www.fda.gov/Food/FoodScienceResearch/SafePracticesforFoodProcesses/ucm101662.htm>
- Vautier, M., Guillard, C., Herrmann, J. M., 2001. Photocatalytic degradation of dyes in water: Case study of indigo and of indigo carmine. *J. Catal.*, 201, 46–59.
- Wei, C., Lin, W., Zainal, Z., Williams, N., Zhu, K., Kruzic, A., Smith, R., Rajeshwar, K., 1994. Bactericidal activity of TiO<sub>2</sub> photocatalyst in aqueous media: toward a solar-assisted water disinfection system. *Environ. Sci. Technol.*, 28, 934-938.
- Wolfrum, E., Huang, J., Blake, D., Maness, P., Huang, Z., Fiest, J., 2002. Photocatalytic oxidation of bacteria, bacterial and fungal spores, and model biofilm components to carbon dioxide on titanium dioxide-coated surfaces. *Environ. Sci. Technol.*, 36, 3412-3419.
- Wu, P., Xie, R., Imlay, J., Shang, J., 2008. Visible-light-induced photocatalytic inactivation of bacteria by composite photocatalysts of palladium oxide and nitrogen-doped titanium oxide. *Appl. Catal. B-Environ.*, 88 (3-4), 576-581.

- Ye, F., & Ohmori, A., 2002. The photocatalytic activity and photo-absorption of plasma sprayed  $\text{TiO}_2\text{-Fe}_3\text{O}_4$  binary oxide coatings. *Surface and Coatings Technology*, 160, pp. 62–6.
- Zanoni, M. V. B., Sene, J. J., Anderson, M. A., 2003. Photoelectrocatalytic degradation of Remazol Brilliant Orange 3R on titanium dioxide thin-film electrodes. *J. Photochem. Photobiol. A*, 157, 55–63.
- Zhou, X., Ji, H., Huang, X., 2012. Photocatalytic degradation of methyl orange over metalloporphyrins supported on  $\text{TiO}_2$  degussa P25. *Molecules*, 17, 1149–1158.